

Adsorbed leucaena protein on citrate modified Fe₃O₄ nanoparticles: synthesis, characterization, and its application as magnetic coagulant

Hans Kristianto (✉ hans.kristianto@unpar.ac.id)

Universitas Katolik Parahyangan Fakultas Teknologi Industri <https://orcid.org/0000-0003-4747-4361>

Edwin Reynaldi

Universitas Katolik Parahyangan Fakultas Teknologi Industri

Susiana Prasetyo

Universitas Katolik Parahyangan Fakultas Teknologi Industri

Asaf K Sugih

Universitas Katolik Parahyangan Fakultas Teknologi Industri

Research

Keywords: Congo red, Fe3O4, iron oxide nanoparticles, Leucaena leucocephala, magnetic coagulant, natural coagulant

Posted Date: December 11th, 2020

DOI: <https://doi.org/10.21203/rs.3.rs-41412/v4>

License:  This work is licensed under a Creative Commons Attribution 4.0 International License.

[Read Full License](#)

Version of Record: A version of this preprint was published at Sustainable Environment Research on December 11th, 2020. See the published version at <https://doi.org/10.1186/s42834-020-00074-4>.

Abstract

Natural coagulants from plants resources have gained a lot of attention as it is renewable, biodegradable, non-hazardous, lower cost, and less sludge generated compared to chemical coagulants. However there are still some drawbacks, namely long settling time and possible increase of dissolved organic carbon in the treated water. In this paper we tried to address these drawbacks by utilizing citrate modified Fe_3O_4 to adsorb protein from *Leucaena leucocephala* as the active coagulating agent. The effect of trisodium citrate concentration and protein adsorption pH to the adsorbed protein was investigated. It was found that the trisodium citrate concentration of 0.5 M and pH 4.0 gave the highest protein adsorption. The obtained magnetic coagulant was furthermore characterized using *Scanning Electron Microscopy*, *X-ray Diffraction*, Fourier Transform *Infrared Spectroscopy*, and *Transmission Electron Microscopy* to observe the characteristics before and after protein adsorption. Furthermore, the effect of pH (2 to 10) and coagulant dosage (60 to 600 mg L⁻¹) to the removal of synthetic Congo red wastewater and sludge volume formation was investigated. It was found that pH 3 was the best pH for coagulation due to charge neutralization mechanism of leucaena protein. Furthermore the highest removal was obtained at dosage 420 mg L⁻¹ with 80% removal. This result was comparable with crude extract of leucaena with half settling time (20 min) and lower increase of permanganate value, indicating lower increase of dissolved organics in the treated water.

1. Introduction

In recent years, utilization of various natural resources as natural coagulant has gained a lot of interest due to its various advantages, such as: lower cost compared to chemical coagulants, it comes from renewable sources, less sludge volume generated, and biodegradable- non-hazardous sludge [1, 2]. However there are some drawbacks in natural coagulant application, which we addressed in this research. Firstly, the settling time needed for separation of flocs is most likely between 60 to 120 min by gravity. It is important to decrease the settling time, as long residence time could lead to larger designed settling tank needed, which could lead to higher capital cost. Secondly, direct utilization of plant parts or its crude extract could increase the dissolved organic carbon (DOC) in the treated water, due to some soluble non-coagulant compounds from the plant [3]. It is known that high DOC could stimulate high microbial activities, making disinfection process more difficult.

There were some researchers that combined iron oxide nanoparticles and natural coagulant to improve the coagulation performance, especially in terms of settling time [4-10]. There are two approaches that have been used, firstly the protein as active coagulating agent was used to functionalize the surface of iron oxide nanoparticles, secondly, the iron oxide nanoparticles were dispersed in crude extract of natural coagulant. Okoli et al. [4] synthesized magnetic coagulant using composite of Fe_3O_4 and $\gamma\text{-Fe}_2\text{O}_3$ water-oil emulsion and functionalized with purified protein from *Moringa oleifera*. It was reported that 90% turbidity removal was obtained at 12 min settling under external magnet force, compared to gravitation only (240 min).

Different types of iron oxide nanoparticles, α -Fe₂O₃, γ -Fe₂O₃, and Fe₃O₄, have been studied by Santos group to remove turbidity and color from synthetic wastewater [5-9]. In those researches, iron oxide nanoparticles were dispersed in crude extract of *M. oleifera*, where it was found that significant removal of turbidity and color was achieved within short settling time (less than 30 min) under magnetic settling. It was also found that the coagulation mechanism was mostly charge neutralization, where protein acted as the active coagulating agent, and interaction between protein and iron oxide nanoparticles made the fast settling process possible. Similar result was also obtained in our previous study [10] where magnetically assisted coagulation of Congo red gave half settling time when compared to leucaena extract only with similar removal value. Vieira group isolated globulin and albumin fraction from *M. oleifera* and functionalized it with iron oxide nanoparticles [11, 12]. The obtained magnetic coagulant was used to remove color from synthetic dye waste namely Amaranth, Brilliant Blue, Sunset Yellow, and Reactive Black 5. Combination of albumin and iron oxide nanoparticles gave color removal around 52-94%, depending to the dyes, with 5 min magnetic sedimentation.

Concerning the high DOC content of natural coagulant treated water; some efforts have been done by previous researchers. Yin [1] suggested that extraction and isolation of active coagulating agent could tackle this problem. Extraction of active coagulating agent, especially protein, using saline has been extensively studied. It has been proven that salting-in interaction between NaCl and protein could increase the protein solubility, resulting in lower dosage needed in the coagulation. This extraction step could be followed by purification steps to isolate protein that acts as active coagulating agent. Several purification methods have been investigated, such as ion exchange [13-15], dialysis [16], spray drying [17], ultrafiltration [18, 19], and lyophilization [20]. However, the previously mentioned methods require many complicated steps, making it impractical in large scale.

Iron oxide nanoparticles are known to be able to selectively bind protein thus could be used in protein purification [21]. However, for its application in aqueous medium, the hydrophobicity of iron oxide nanoparticles becomes its drawback [22]. On the other hand, the presence of hydroxyl group on the surface of iron oxide nanoparticles makes the surface of particles easily modified using various functional groups, one of which is carboxylic acid [23]. Citric acid, a trivalent organic acid, has been widely used as capping agent to prevent agglomeration of iron nanoparticles. Furthermore, citric acid modified iron oxide nanoparticles has shown affinity for immobilize protein, enzymes, drugs, etc. [24-29].

In this study, we investigate functionalized Fe₃O₄ nanoparticles with protein from leucaena (*Leucaena leucocephala*) crude extract as magnetic natural coagulant to treat synthetic Congo red wastewater. To the best of authors' knowledge, this study is the first study that reported utilization of adsorbed protein on citrate modified Fe₃O₄ as magnetic coagulant. Based on our previous study, leucaena protein could act as natural coagulant to remove turbidity [30] and color [31]. The Fe₃O₄ was modified using citrate ion that acted as a bridge for protein adsorption. The effect of pH modification and citrate ion concentration to the protein adsorbed was investigated. The best condition that gave the highest adsorbed protein was characterized and used as magnetic coagulant for Congo red removal from synthetic wastewater. The effects of coagulation pH, magnetic coagulant dosage, and removal kinetics under magnetic field were

investigated. Furthermore, the changes of DOC in the wastewater before and after coagulation using magnetic coagulant and crude extract were estimated using permanganate value (PV).

2. Materials And Methods

2.1. Synthesis of magnetic coagulant

The synthesis of magnetic coagulant was following the method used by Rahman et al. [27] with modification. A mixture of 80 mg Fe_3O_4 (pure grade, Sigma Aldrich) and 160 mL trisodium citrate (pure grade, Sigma Aldrich) was sonicated for 30 min, followed by mixing for 2 h at 80 °C. The mixture was let cool to room temperature, then separated using magnet, and washed using distilled water to remove unadsorbed citrate anion. The citrate modified Fe_3O_4 , denoted as $\text{Fe}_3\text{O}_4\text{-CA}$, was then oven dried in vacuum condition at 60 °C, and then stored in a closed lid in a desiccator.

Leucaena protein was used as the protein source to functionalize the $\text{Fe}_3\text{O}_4\text{-CA}$. Dried leucaena seeds were obtained from Probolinggo, East Java. The seeds kernel was separated from its coat by grinding and sieving. Furthermore, the seeds kernel was grinded and sieved using a standard mesh to obtain seeds kernel powder with size smaller than 0.177 mm (80 mesh). Extraction of protein from seeds kernel powder was done by using 1 M NaCl solution with seeds to solvent mass ratio of 1:20 using dispersed batch method for 60 min. The cake was separated by mean of filtration, and the extract was used for $\text{Fe}_3\text{O}_4\text{-CA}$ functionalization. To prevent any degradation during storage, the extract was freshly made prior to every experiment. Observation of leucaena isoelectric point (pl) was done by similar extraction procedure with variations of initial pH (2 to 9), adjusted using 0.1 M HCl or NaOH solution. The extracted protein concentration in the solution was determined using Bradford method [32].

Functionalization of $\text{Fe}_3\text{O}_4\text{-CA}$ was done by mixing 5 mL of leucaena crude extract, in which pH was adjusted using 0.1 M citrate buffer solution, prior to mixing with 80 mg $\text{Fe}_3\text{O}_4\text{-CA}$. The mixture was sonicated for 1 min, followed by mixing at room temperature for 4 h. The protein functionalized iron nanoparticles, denoted as $\text{Fe}_3\text{O}_4\text{-CA-protein}$, was separated using external magnet, washed with distilled water, and vacuum dried at 60 °C. The obtained $\text{Fe}_3\text{O}_4\text{-CA-protein}$ was stored in a closed lid in a desiccator.

The functionalization of $\text{Fe}_3\text{O}_4\text{-CA}$ was first done at various pH (3 to 6) at constant trisodium citrate concentration of 0.5 M to observe the effect of pH to the protein adsorption. Furthermore, the effect of trisodium citrate concentration was studied at the best pH by varying trisodium citrate concentration (0 to 1.0 M). The protein concentration in the solution before and after adsorption was determined using Bradford method [32], where the protein concentration was stated equivalent to bovine serum albumin (BSA) standard. The response observed was the protein adsorption capacity (q ; mg eq BSA mg^{-1} Fe_3O_4), which was calculated using Eq. (1), where C_t and C_e (mg eq BSA L^{-1}) were initial and final protein concentration, m (mg) is the mass of Fe_3O_4 , and V (L) is the volume of the solution. The obtained $\text{Fe}_3\text{O}_4\text{-}$

CA-protein with highest protein adsorption capacity was further characterized and used as magnetic coagulant in this study.

$$q = \frac{(ct-ce) \times V}{m} \quad (1)$$

2.2. Characterization

The magnetic coagulant that gave the highest protein adsorption was characterized to observe the difference before and after protein functionalization. Determination of point of zero charge (pH_{pzc}) of pristine and citrate modified Fe_3O_4 was done using pH drift method [33]. The functional groups of pristine Fe_3O_4 , citrate modified Fe_3O_4 , and protein functionalized Fe_3O_4 were characterized using KBr pellet method Fourier Transform Infrared Spectroscopy (FTIR; Prestige 21 Shimadzu Instruments). The morphology was observed using Scanning Electron Microscope (SEM; Hitachi SU3500). The particle size was observed using Transmission Electron Microscope (TEM; Hitachi HT7700), while the crystallinity was analyzed using X-Ray Diffraction (XRD; Bruker D8 Advance). Based on the XRD spectra, the crystallite size (d in nm) was estimated using Scherrer equation (Eq. (2)), where θ is the Bragg angle; K is Scherrer constant (0.9); λ (nm) is the wavelength of Cu K- α radiation (0.15405 nm); and β is the full width at half maximum peak.

$$d = \frac{K\lambda}{\beta \cdot \cos\theta} \quad (2)$$

2.3. Jar test experiment

The obtained magnetic coagulant was tested to remove synthetic dye wastewater. Congo red (Aldrich) dissolved in distilled water with concentration of 10 ppm was used as the model dye in this study. Coagulation study was done by mixing magnetic coagulant and Congo red solution with rapid mixing at 100 rpm for 2 min, followed by slow mixing at 20 rpm for 20 min using a jar test apparatus. The mixture was then let to settle in an Imhoff cone under array of neodymium magnets. During this step, sample of treated water was taken every 5 min until 1 h. The concentration of Congo red at initial condition and during sampling was measured using a spectrophotometer at its maximum wavelength (505 nm). The removal of Congo red was calculated using Eq. (3), where A_i and A_f are initial and final absorbance, respectively. The sludge volume (mL L^{-1}) was measured using Imhoff cone after 1 h settling, and calculated using Eq. (4). The effect of pH to the coagulation was observed by varying the wastewater pH (2 to 10) at constant dosage of 60 mg L^{-1} . Furthermore, the study of magnetic coagulant dosage's effect to coagulation was done at best pH at various coagulant dosages (60 to 600 mg L^{-1}).

$$\% \text{ removal} = \frac{A_i - A_f}{A_i} \times 100\% \quad (3)$$

$$\text{sludge volume} = \frac{\text{sludge volume (mL)}}{\text{wastewater volume (L)}} \quad (4)$$

The PV was measured at the best pH and coagulant dosage using following method [34]: 5 mL of 4 N H₂SO₄ and 10 mL of 0.1 N KMnO₄ were added into 100 mL of sample solution. The mixture was heated for 10 min, after which 10 mL of 0.01 N H₂C₂O₄ solutions was added. The solution is back titrated using KMnO₄ solution until the end point was reached. The volume titration of the potassium permanganate solution used was recorded, and the PV (mg KMnO₄ L⁻¹) was calculated.

2.4. Settling kinetic models

The evaluation of removal during settling was approached using several adsorption kinetic models. The value of adsorption capacity, q (mg dye mg magnetic coagulant⁻¹), was calculated using Eq. (1).

The kinetic models used in this study are pseudo-first order, pseudo-second order, Elovich, and intra-particle diffusion models, where the linearized form for each model is presented in Eqs. (5) to (8) [35], respectively. The q_t and q_e values in those equations represent adsorption capacity (mg dye g⁻¹ magnetic coagulant) as function of time (min) and at equilibrium. Constant k_1 (min⁻¹) represents pseudo first-order rate constant; k_2 (mg dye g⁻¹ magnetic coagulant min⁻¹) is the pseudo second-order rate constant; and k_d (mg dye g⁻¹ magnetic coagulant min^{-1/2}) is the rate constant for intra-particle diffusion model. The value α denotes initial adsorption rate (mg dye g⁻¹ magnetic coagulant min⁻¹) and β (mg magnetic coagulant g⁻¹ dye) is the activation energy related value of chemisorption for Elovich model.

$$\ln(q_e - q_t) = \ln(q_e) - k_1 t \quad (5)$$

$$\frac{t}{q_t} = \frac{t}{q_e} + \frac{1}{k_2 q_e^2} \quad (6)$$

$$q_t = \frac{1}{\beta} \ln(\alpha\beta) + \frac{1}{\beta} \ln(t) \quad (7)$$

$$q_t = k_d t^{1/2} \quad (8)$$

3. Results And Discussion

3.1. Effect of pH and trisodium citrate concentration on the protein adsorption

As mentioned before, the citrate ion was used as a bridge between Fe₃O₄ and leucaena protein, making the adsorption process effectively. The effect of adsorption pH and trisodium citrate concentration is presented in Figs. 1a and 1b. It could be observed in Fig. 1a, that pH played an important role in protein adsorption. With the increase of adsorption pH from 3.0 to 4.0, the leucaena protein adsorption capacity was also increased and reached the highest adsorption capacity at pH 4.0. Further increase of adsorption pH to 6.0 led to the decrease of protein adsorption. It is known that electrostatic force plays an important role in protein adsorption. From the pH_{pzc} (Fig. 1c), it could be observed that citrate modified Fe₃O₄ had lower pI (around 3.9), compared to the pristine one (around 7.1). This result is consistent with previous

research [36]. On the other hand, the leucaena protein's *pI* was estimated around pH 4 (Fig. 1d), where the protein solubility is at its minimum [37]. At low pH, both Fe_3O_4 and leucaena protein had positive charges, thus repulsive forces between them making low adsorption. Similar phenomenon was possibly happened at pH above 4.0. The highest protein adsorption capacity was obtained at pH 4.0, which was near *pI* of leucaena protein. It is known that at pH near *pI*, the protein structure is at more compact conformation state, lowering repulsion forces between particles thus making higher protein adsorption possible [38]. Similar phenomenon has also been reported before [38, 39].

The effect of trisodium citrate concentration to the protein adsorption was further investigated. It was found that addition of trisodium citrate could increase the protein adsorption capacity. Based on Fig. 1b, it could be observed that the addition of trisodium citrate to 0.5 M increased the protein adsorption. We speculate it is possible due to with increase of citrate ion in the modification process, more citrate ions are adsorbed on Fe_3O_4 surface, making more protein adsorption possible. Further addition of citrate ion did not increase the adsorption capacity, due to all Fe_3O_4 surface already occupied. Similar result was also obtained by previous researchers [27]. Based on these results, the trisodium citrate of 0.5 M and protein adsorption at pH 4.0 were further characterized and used as magnetic coagulant.

3.2. Characterization of Fe-CA-Protein

The characteristics of Fe_3O_4 before and after protein modification are presented in Fig. 2. Based on the SEM observation, the nanoparticles were in form of aggregation of Fe_3O_4 . The functionalization did not give any significant difference to the particle morphology. Similar spectra were also observed for Fe_3O_4 and Fe_3O_4 -CA-protein samples, where both samples exhibited (111), (202), (311), (222), (400), (422), (511), and (440) peaks of magnetite [40]. Further calculation using Scherer equation showed that functionalized Fe_3O_4 had bigger average diameter of 58 nm, compared to pristine Fe_3O_4 (47 nm). Based on the Fe_3O_4 IR spectra, it could be observed that the sample exhibited a Fe-O vibration at 580 cm^{-1} , and peaks at $1613, 3436 \text{ cm}^{-1}$ that came from O-H vibration of water molecule on the crystal structure [41, 42]. After modification using CA, the Fe_3O_4 -CA sample exhibited stronger peak at 1620 and 3436 cm^{-1} indicating symmetric stretching of C=O and O-H vibration from CA molecules that adsorbed on the surface of Fe_3O_4 . After adsorption of protein, there are several peaks that could be observed: 1397 cm^{-1} bending vibration of C-H bonds, $\sim 1600 \text{ cm}^{-1}$ peak of N-H bending, while peaks around 3200 - 3400 cm^{-1} came from overlap of O-H and N-H stretching [27, 43]. The observed peaks indicated that protein from leucaena crude extract has been adsorbed on the surface of modified Fe_3O_4 . The presence of coating of protein on Fe_3O_4 was visible in TEM image (Fig. 2f, white arrow), compared to pristine Fe_3O_4 .

3.3. Effect of pH in coagulation

The effect of pH in the coagulation process is presented in Fig. 3. It could be observed that there was increase of removal from pH 2 to 3, and the highest removal of Congo red was obtained at pH 3. Very low removal was obtained while increasing the pH from 4 to 10, indicating no coagulation process happened.

The leucaena protein on magnetic coagulant possessed *pI* around 4, thus at pH below 4, the magnetic coagulant would be positively charged. This charge was the opposite of Congo red molecules, which is known to be negatively charged at pH ≥ 3 , making the coagulation process possible through charge neutralization mechanism. At pH 2, low coagulation performance was due to denaturation of protein molecules on the magnetic coagulant. Denaturation of protein is commonly observed at extremely low pH [44], making it inactive for coagulation process. On the other hand, at pH above leucaena protein *pI* value, both the coagulant and Congo red molecules were positively charge, thus no coagulation occurred at these conditions. Along with the increase of destabilized Congo red molecules, the more sludge volume was generated, as observed in pH 3. As very low removal was observed at pH 4-10, minimum destabilization was occurred, resulting in no observed sludge. Similar result was obtained in our previous studies using leucaena crude extract as natural coagulant, where pH 3 was the best pH for coagulation [10, 31].

3.4. Effect of magnetic coagulant dosage

The study of magnetic coagulant dosage was done at pH 3, which was found as the best pH for coagulation. The profile of % removal and sludge volume at various dosages is presented in Fig. 4. At low coagulant dosage, there was insufficient coagulant to neutralize the Congo red molecules, resulting on low removal. With increase of magnetic coagulant dosage, the removal was also increased until dosage of 420 mg L^{-1} . Further increase of magnetic coagulant dosage to 600 mg L^{-1} did not give any significant increase to the removal of Congo red. This was possible due to over addition of coagulant limiting the adsorption efficiency, as the magnetic coagulant particle could aggregate to each other [45] lowering the coagulation efficiency. Furthermore colloid re-stabilization is known to be commonly happened under over addition of coagulant [46]. This phenomenon could decrease the removal efficiency. Similar trend was also observed for the sludge volume.

The Congo red removal as function of time is presented in Fig. 5. Comparison experiments were done using only leucaena crude extract and Fe_3O_4 with concentration of $370 \text{ mg eq BSA L}^{-1}$ and 50 mg L^{-1} respectively, proportional to the adsorbed protein at the best magnetic coagulant dosage (420 mg L^{-1}). It could be observed that significant removal was obtained at the first 20 min and became relatively constant until 60 min. This observation showed the significance of Fe_3O_4 in the magnetic coagulant that increased the removal kinetics, compared to leucaena crude extract that need 40 min before reached constant. It could be also observed in Fig. 5b, the Fe_3O_4 did not contribute to the Congo red removal, indicating the leucaena protein was the active coagulating agent.

The Congo red removal kinetics was further investigated using various kinetic models, namely: pseudo 1st order, pseudo 2nd order, Elovich, and interparticle diffusion models. It is known that coagulation mechanism in this study was charge neutralization which is usually preceded by adsorption of dye molecules on active coagulating agent. The adsorption step usually becomes the rate determining step in coagulation study, making adsorption models suitable for removal evaluation [47]. According to Obiora-Okafo et al. [48], this phenomenon is possible due to the polymeric nature of natural coagulants. The

fitting result of various kinetic models is presented in Table 1, and sample of model plots is presented in Fig. 6. Based on the R^2 value, it could be seen that pseudo 2nd order kinetics was highly suitable for kinetics modeling with R^2 value of 0.99, while the Elovich and intra-particle diffusion models also gave good model-data correlation with R^2 value around 0.70 to 0.90. Suitability of the pseudo 2nd order and Elovich kinetics to the removal of Congo red implied that the adsorption occurred during coagulation was chemisorption. It was possible due to the different charges between proteins on the magnetic coagulant and the Congo red molecules, making dipole-dipole interaction possible [49]. A 2-phase plot was observed in the interparticle diffusion model (Fig. 6d), indicating there are 2 determining step, namely surface adsorption followed by intra-particle diffusion. Similar conclusions of removal kinetic were also obtained in previous researches [6, 10, 50, 51].

Based on the characterization results and suitability of the kinetic models, an illustration of coagulation mechanism is presented in Fig. 7. One of $-COOH$ of citrate ions was adsorbed to the surface of Fe_3O_4 , while the others were available for protein binding. The overall magnetic coagulant was positively charged, following the charge of leucaena protein adsorbed on Fe_3O_4 -CA, thus neutralizing the negatively charged Congo red molecules. The measurement of PV was done at the best magnetic coagulant condition (pH 3, dosage of 420 mg L^{-1}). Initial Congo red wastewater had PV of $8.6\text{ mg KMnO}_4\text{ L}^{-1}$, and water treated using leucaena crude extract showed $15.0\text{ mg KMnO}_4\text{ L}^{-1}$ (increase of 49%). This increase was possible due to the presence of various soluble organic compounds in the crude extract. The magnetic coagulant showed lower increase of PV (18%), compared to the leucaena crude extract, due to desorbed protein in the treated wastewater.

4. Conclusions

This study focused on synthesis of magnetic coagulant by means of leucaena protein adsorption on the surface of citrate modified Fe_3O_4 . Various trisodium citrate concentration and protein adsorption pH was investigated. Trisodium citrate was found to act as bridge between Fe_3O_4 and protein molecules, where at concentration of 0.5 M and pH 4.0, the highest protein adsorption was achieved. Further trisodium citrate concentration did not give any increase in protein adsorption. The functionalization of Fe_3O_4 did not change the morphology and crystallinity, however, bigger average crystal size was observed after protein functionalization. The adsorption of citrate and protein on the surface of Fe_3O_4 was confirmed by using FTIR analysis. The obtained magnetic coagulant was tested for its coagulation performance. At various coagulation pH, the highest removal was obtained at pH 3, indicating charge neutralization mechanism due to the positively charged protein at pH around 3. At various magnetic coagulant dosages, the increase of magnetic coagulant dosage increased the removal of Congo red, until the highest removal at 420 mg L^{-1} . Further increase did not give any effect to the removal. From investigation using several kinetic models, it was found that the removal kinetic was well fitted with pseudo 2nd order kinetic model, reflected in high R^2 value (> 0.99). The best coagulation was obtained at pH 3 and dosage of 420 mg L^{-1} with 80% removal. This result was comparable with crude extract of leucaena with half settling time (20

min) and lower increase of permanganate value. While this preliminary study shows that leucaena protein adsorbed on citrate modified Fe_3O_4 system may serve as a promising coagulant, further research is needed before this natural coagulant can be utilized for practical applications. Further systematic experiments to study the effect of several parameters affecting coagulation in real wastewater, such as conductivity of various background ions and wastewater temperature will be carried out, and the results will be reported in the forthcoming papers.

Declarations

Availability of data and materials

All data generated or analyzed during this study are included in this article. The raw data are available from the corresponding author upon reasonable request.

Competing interests

The authors declare they have no competing interests.

Funding

This work was supported by Parahyangan Catholic University Centre of Research and Community Service with contract No III/LPPM/2020-01/09-P.

Authors' contributions

ER and HK carried out laboratory experimental studies and drafted the manuscript. HK, SP, and AKS designed the study and secured the funding. SP and AKS critically reviewed and edited the final manuscript. All the authors read and approved the final manuscript.

Acknowledgements

The authors acknowledged financial support by Parahyangan Catholic University Centre of Research and Community Service with contract No III/LPPM/2020-01/09-P. The authors also wish to thank all who have assisted in conducting this study.

References

1. Yin CY. Emerging usage of plant-based coagulants for water and wastewater treatment. *Process Biochem.* 2010;45:1437–
2. Saleem M, Bachmann RT. A contemporary review on plant-based coagulants for applications in water treatment. *J Ind Eng Chem.* 2019;72:281-97.
3. Ramavandi B. Treatment of water turbidity and bacteria by using a coagulant extracted from *Plantago ovata*. *Water Resour Ind.* 2014;6:36–

4. Okoli C, Boutonnet M, Jaras S, Rajarao-Kuttuva G. Protein-functionalized magnetic iron oxide nanoparticles: time efficient potential-water treatment. *J Nanopart Res.* 2012;14:1194.
5. Mateus GAP, Paludo MP, dos Santos TRT, Silva MF, Nishi L, Fagundes-Klen MR, et al. Obtaining drinking water using a magnetic coagulant composed of magnetite nanoparticles functionalized with *Moringa oleifera* seed extract. *J Environ Chem Eng.* 2018;6:4084-92.
6. Mateus GAP, dos Santos TRT, Sanches IS, Silva MF, de Andrade MB, Paludo MP, et al. Evaluation of a magnetic coagulant based on Fe_3O_4 nanoparticles and *Moringa oleifera* extract on tartrazine removal: coagulation-adsorption and kinetics studies. *Environ Technol* 2020;41:1648-63.
7. Santos TRT, Silva MF, Nishi L, Vieira AMS, Klein MRF, Andrade MB, et al. Development of a magnetic coagulant based on *Moringa oleifera* seed extract for water treatment. *Environ Sci Pollut R.* 2016;23:7692-700.
8. dos Santos TRT, Mateus GAP, Silva MF, Miyashiro CS, Nishi L, de Andrade MB, et al. Evaluation of magnetic coagulant ($\alpha\text{-Fe}_2\text{O}_3\text{-MO}$) and its reuse in textile wastewater treatment. *Water Air Soil Pollut.* 2018;229:92.
9. dos Santos TRT, Silva MF, de Andrade MB, Vieira MF, Bergamasco R. Magnetic coagulant based on *Moringa oleifera* seeds extract and super paramagnetic nanoparticles: optimization of operational conditions and reuse evaluation. *Desalin Water Treat.* 2018;106:226-37.
10. Kristianto H, Tanuarto MY, Prasetyo S, Sugih AK. Magnetically assisted coagulation using iron oxide nanoparticles-*Leucaena leucocephala* seeds' extract to treat synthetic Congo red wastewater. *Int J Environ Sci Te.* 2020;17:3561-70.
11. Reck IM, Baptista ATA, Paixao RM, Bergamasco R, Vieira MF, Vieira AMS. Application of magnetic coagulant based on fractionated protein of *Moringa oleifera* seeds for aqueous solutions treatment containing synthetic dyes. *Environ Sci Pollut R.* 2020;27:12192-201.
12. Reck IM, Baptista ATA, Paixao RM, Bergamasco R, Vieira MF, Vieira AMS. Protein fractionation of *Moringa oleifera* seeds and functionalization with magnetic particles for the treatment of reactive black 5 solution. *Can J Chem Eng.* 2019;97:2309-17.
13. Ghebremichael KA, Gunaratna KR, Dalhammar G. Single-step ion exchange purification of the coagulant protein from *Moringa oleifera*. *Appl Microbiol Biot.* 2006;70:526-32.
14. Ghebremichael K. Overcoming the drawbacks of natural coagulants for drinking water treatment. *Water Supply.* 2007;7:87-93.
15. Sanchez-Martin J, Ghebremichael K, Beltran-Heredia J. Comparison of single-step and two-step purified coagulants from *Moringa oleifera* seed for turbidity and DOC removal. *Bioresour Technol.* 2010;101:6259-61.
16. Dezfooli SM, Uversky VN, Saleem M, Baharudin FS, Hitam SMS, Bachmann RT. A simplified method for the purification of an intrinsically disordered coagulant protein from defatted *Moringa oleifera*. *Process Biochem.* 2016;51:1085-91.
17. Mohammad TA, Mohamed EH, Megat Mohd Noor MJ, Ghazali AH. Coagulation activity of spray dried salt extracted *Moringa oleifera*. *Desalin Water Treat.* 2013;51:1941-6.

18. Antov MG, Sciban MB, Prodanovic JM. Evaluation of the efficiency of natural coagulant obtained by ultrafiltration of common bean seed extract in water turbidity removal. *Ecol Eng.* 2012;49:48-52.
19. Prodanovic JM, Antov MG, Sciban MB, Ikonic BB, Kukic DV, Vasic VM, et al. The fractionation of natural coagulant extracted from common bean by use of ultrafiltration membranes. *Desalin Water Treat.* 2013;51:442-7.
20. Mohamed EH, Mohammad TA, Noor MJMM, Ghazali AH. Influence of extraction and freeze-drying durations on the effectiveness of *Moringa oleifera* seeds powder as a natural coagulant. *Desalin Water Treat.* 2015;55:3628-34.
21. Okoli C, Fornara A, Qin J, Toprak MS, Dalhammar G, Muhammed M, et al. Characterization of superparamagnetic iron oxide nanoparticles and its application in protein purification. *J Nanosci Nanotechno.* 2011;11:10201-6.
22. Mahdavinia GR, Etemadi H. Surface modification of iron oxide nanoparticles with κ-carrageenan/carboxymethyl chitosan for effective adsorption of bovine serum albumin. *Arab J Chem.* 2019;12:3692-703.
23. Boyer C, Whittaker MR, Bulmus V, Liu JQ, Davis TP. The design and utility of polymer-stabilized iron-oxide nanoparticles for nanomedicine applications. *NPG Asia Mater.* 2010;2:23-30.
24. Nosrati H, Adibtabar M, Sharafi A, Danafar H, Kheiri MH. PAMAM-modified citric acid-coated magnetic nanoparticles as pH sensitive biocompatible carrier against human breast cancer cells. *Drug Dev Ind Pharm.* 2018;44:1377-84.
25. Patel U, Chauhan K, Gupte S. Synthesis, characterization and application of lipase-conjugated citric acid-coated magnetic nanoparticles for ester synthesis using waste frying oil. *3 Biotech.* 2018;8:211.
26. Cahyana AH, Pratiwi D, Ardiansah B. Citrate-capped superparamagnetic iron oxide (Fe_3O_4 -CA) nanocatalyst for synthesis of pyrimidine derivative compound as antioxidative agent. *IOP Conf Ser Mat Sci.* 2017;188:012008.
27. Rahman ZU, Dong YL, Ren CL, Zhang ZY, Chen XG. Protein adsorption on citrate modified magnetic nanoparticles. *J Nanosci Nanotechno.* 2012;12:2598-606.
28. Lesiak B, Rangam N, Jiricek P, Gordeev I, Toth J, Kover L, et al. Surface study of Fe_3O_4 nanoparticles functionalized with biocompatible adsorbed molecules. *Front Chem.* 2019;7:642.
29. Vinambres M, Filice M, Marciello M. Modulation of the catalytic properties of lipase b from *Candida antarctica* by immobilization on tailor-made magnetic iron oxide nanoparticles: the key role of nanocarrier surface engineering. *Polymers-Basel.* 2018;10:615.
30. Kristianto H, Paulina S, Soetedjo JNM. Exploration of various Indonesian indigenous plants as natural coagulants for synthetic turbid water. *Int J Technol.* 2018;9:464-71.
31. Kristianto H, Rahman H, Prasetyo S, Sugih AK. Removal of Congo red aqueous solution using *Leucaena leucocephala* seed's extract as natural coagulant. *Appl Water Sci.* 2019;9:88.
32. Bradford MM. A rapid and sensitive method for the quantitation of microgram quantities of protein utilizing the principle of protein-dye binding. *Anal Biochem.* 1976;72:248–54.

33. Stan M, Lung I, Soran ML, Opris O, Leostean C, Popa A, et al. Data on the removal of Optilan Blue dye from aqueous media using starch-coated green synthesized magnetite nanoparticles. *Data Brief*. 2019;25:104165.
34. Maidment C, Mitchell P, Westlake A. Measuring aquatic organic pollution by the permanganate value method. *J Biol Educ*. 1997;31:126-30.
35. Riahi K, Chaabane S, Ben Thayer B. A kinetic modeling study of phosphate adsorption onto *Phoenix dactylifera* date palm fibers in batch mode. *J Saudi Chem Soc*. 2017;21:S143-52.
36. Liu JJ, Dai C, Hu YD. Aqueous aggregation behavior of citric acid coated magnetite nanoparticles: effects of pH, cations, anions, and humic acid. *Environ Res*. 2018;161:49-60.
37. Swamylingappa B, Srinivas H. Preparation and properties of protein isolate from hexane-acetic acid treated commercial soybean meal. *J Agr Food Chem*. 1994;42:2907-11.
38. Peng ZG, Hidajat K, Uddin MS. Adsorption of bovine serum albumin on nanosized magnetic particles. *J Colloid Interf Sci*. 2004;271:277-83.
39. Liang YY, Zhang LM, Li W, Chen RF. Polysaccharide-modified iron oxide nanoparticles as an effective magnetic affinity adsorbent for bovine serum albumin. *Colloid Polym Sci*. 2007;285:1193-9.
40. Iida H, Takayanagi K, Nakanishi T, Osaka T. Synthesis of Fe_3O_4 nanoparticles with various sizes and magnetic properties by controlled hydrolysis. *J Colloid Interf Sci*. 2007;314:274-80.
41. Jannah NR, Onggo D. Synthesis of Fe_3O_4 nanoparticles for colour removal of printing ink solution. *J Phys Conf Ser*. 2019;1245:012040.
42. Srivastava V, Singh PK, Weng CH, Sharma YC. Economically viable synthesis of Fe_3O_4 nanoparticles and their characterization. *Pol J Chem Technol*. 2011;13:1-5.
43. Ramzannezhad A, Bahari A. Characteristics of Fe_3O_4 , $\alpha\text{-Fe}_2\text{O}_3$, and $\gamma\text{-Fe}_2\text{O}_3$ nanoparticles as suitable candidates in the field of nanomedicine. *J Supercond Nov Magn*. 2017;30:2165-74.
44. Wu YV, Inglett GE. Denaturation of plant proteins related to functionality and food applications. A review. *J Food Sci*. 1974;39:218-25.
45. Padmavathy KS, Madhu G, Haseena PV. A study on effects of pH, adsorbent dosage, time, initial concentration and adsorption isotherm study for the removal of hexavalent chromium (Cr (VI)) from wastewater by magnetite nanoparticles. *Proc Tech*. 2016;24:585–94.
46. Choy SY, Prasad KMN, Wu TY, Ramanan RN. A review on common vegetables and legumes as promising plant-based natural coagulants in water clarification. *Int J Environ Sci Te*. 2015;12:367-90.
47. Beltran-Heredia J, Sanchez-Martin J, Barrado-Moreno M. Long-chain anionic surfactants in aqueous solution. Removal by *Moringa oleifera*. *Chem Eng J*. 2012;180:128-36.
48. Obiora-Okafo IA, Onukwuli OD, Ezugwu CN. Application of kinetics and mathematical modelling for the study of colour removal from aqueous solution using natural organic polymer. *Desalin Water Treat*. 2019;165:362-73.
49. Jadhav MV, Mahajan YS. Assessment of feasibility of natural coagulants in turbidity removal and modeling of coagulation process. *Desalin Water Treat*. 2014;52:5812-21.

50. Menkiti MC, Okoani AO, Ejimofor MI. Adsorptive study of coagulation treatment of paint wastewater using novel *Brachystegia eurycoma* Appl Water Sci. 2018;8:189.
51. Dalvand A, Nabizadeh R, Ganjali MR, Khoobi M, Nazmara S, Mahvi AH. Modeling of Reactive Blue 19 azo dye removal from colored textile wastewater using L-arginine-functionalized Fe_3O_4 nanoparticles: optimization, reusability, kinetic and equilibrium studies. J Magn Magn Mater. 2016;404:179-89.

Table

Table 1 Kinetics parameter of Congo red removal

	Magnetic coagulant dosage (mg L^{-1})	Pseudo 1st order		Pseudo 2nd order		Elovich		Intra-particle diffusion		
		k_1	R^2	k_2	R^2	α	β	R^2	kd	R^2
60		0.044	0.491	0.027	0.994	246	0.192	0.826	7.0	0.9061
120		0.046	0.4004	0.035	0.9984	1541	0.313	0.7375	7.2	0.9369
180		0.041	0.4664	0.039	0.9983	944	0.345	0.7646	5.5	0.904
240		0.043	0.415	0.050	0.9974	2501	0.437	0.8708	5.4	0.9306
300		0.051	0.5889	0.055	0.9988	4237	0.528	0.7435	4.8	0.9156
360		0.031	0.0126	0.034	0.9984	123	0.349	0.9046	4.5	0.9412
420		0.049	0.4313	0.039	0.9979	149	0.402	0.7797	4.4	0.9652
480		0.033	0.2475	0.044	0.998	70	0.401	0.8236	3.9	0.9694
540		0.029	0.2036	0.043	0.9977	47	0.438	0.8785	3.3	0.9692
600		0.036	0.3235	0.057	0.9983	82	0.529	0.82	3.1	0.9658
370 ^a		0.055	0.4313	0.039	0.9978	7	0.175	0.9674	3.8	0.9818
50 ^b		0.021	0.6233	0.049	0.5314	0.2	0.229	0.9325	0.78	0.7808

^aLeucaena crude extract (mg eq BSA L^{-1}), ^b Fe_3O_4 (mg L^{-1})

Figures

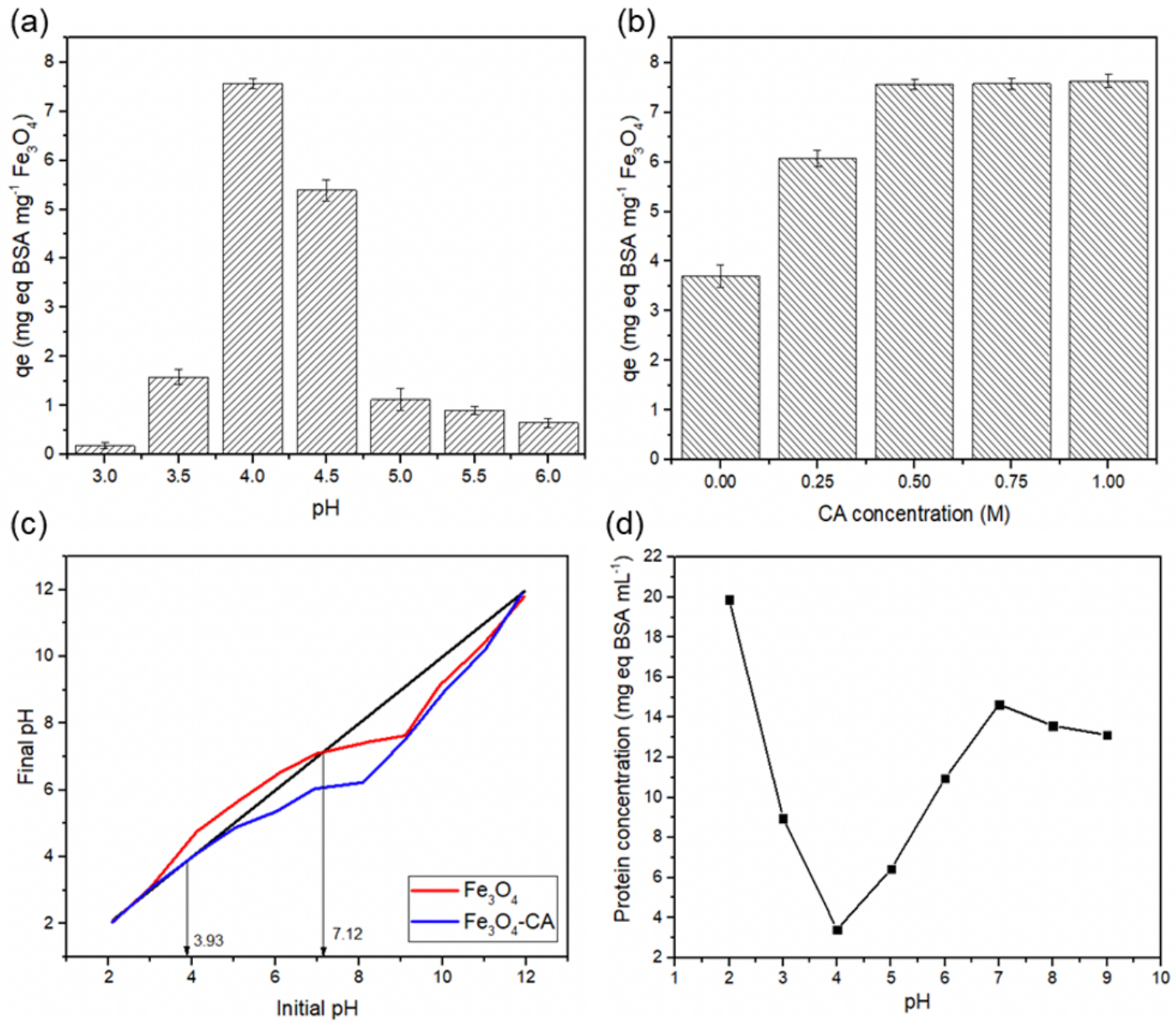


Figure 1

The profile of protein adsorption capacity at various pH (trisodium citrate concentration 0.5 M) (a), various trisodium citrate concentration (protein adsorption at pH 4.0) (b), point of zero charge of Fe_3O_4 and $\text{Fe}_3\text{O}_4\text{-CA}$ (trisodium citrate concentration 0.5 M) (c), and pl of leucaena protein (d)

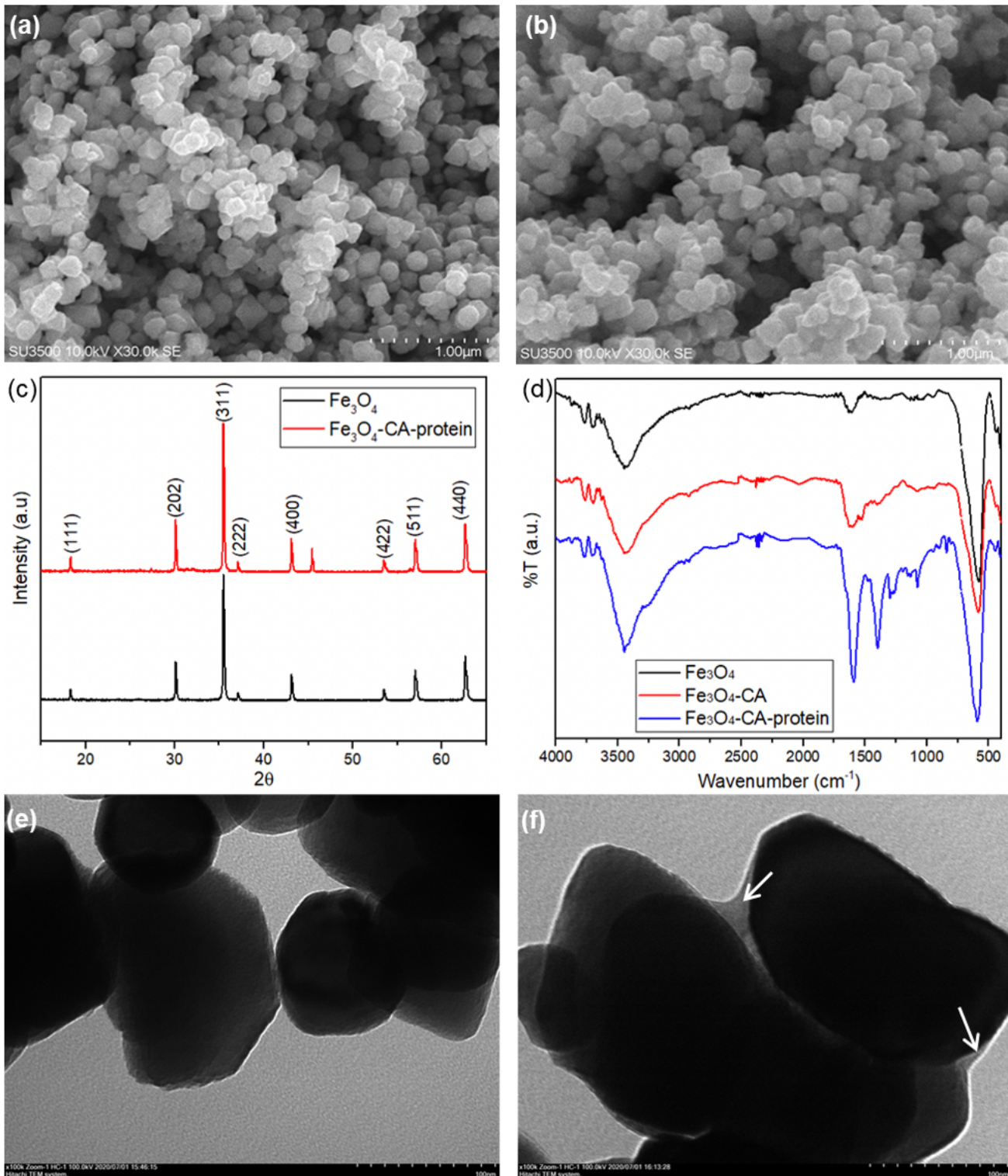


Figure 2

Morphology of Fe₃O₄ (a) and Fe₃O₄-CA-protein (b) at magnification of 30,000×, XRD spectra (c), FTIR spectra (d), and TEM images of Fe₃O₄ (e) and Fe₃O₄-CA-protein (f)

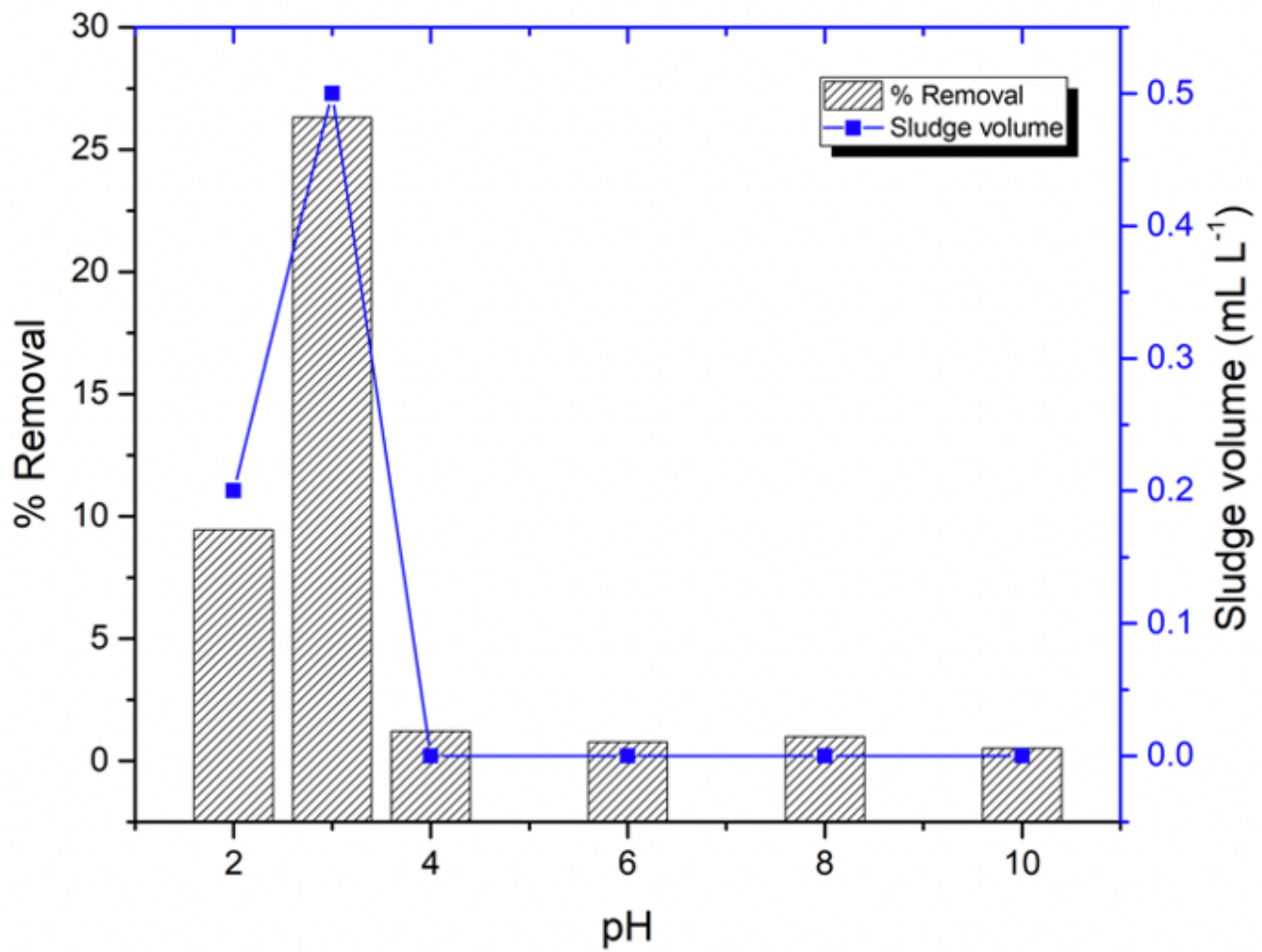


Figure 3

The effect of pH to the coagulation performance (coagulant dosage 60 mg L⁻¹)

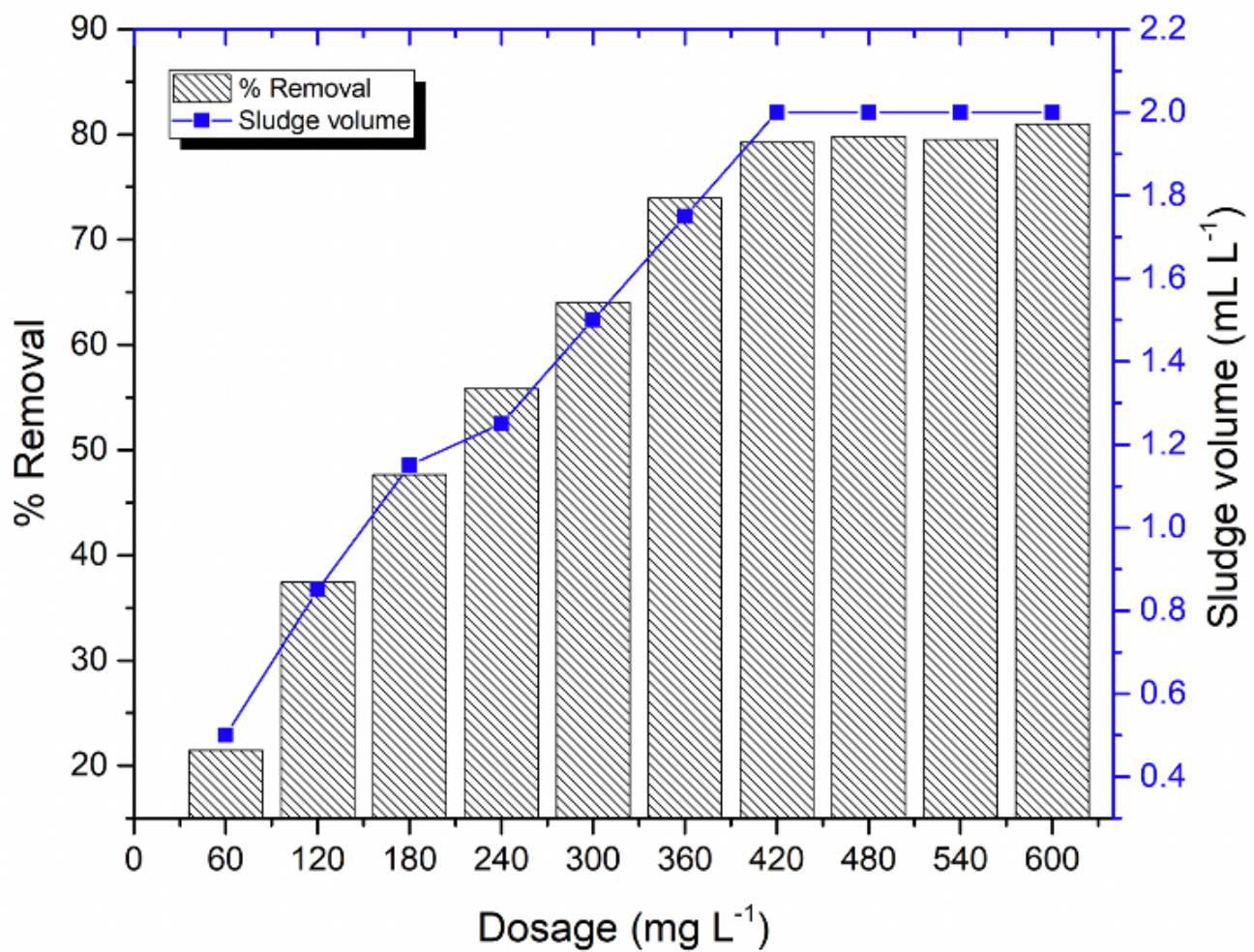


Figure 4

The effect of magnetic coagulant dosage to the coagulation performance

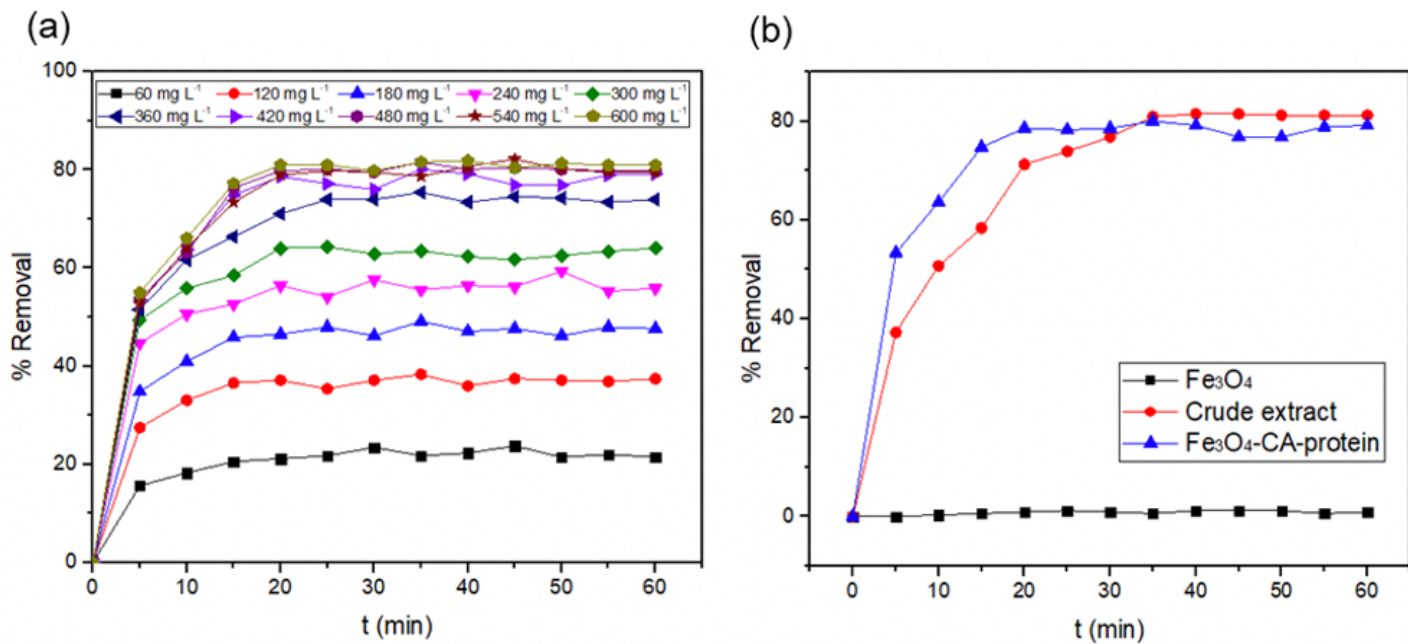


Figure 5

Kinetics parameter of settling at various magnetic coagulant dosages (a) and comparison of magnetic coagulant (Fe₃O₄-CA-protein; 420 mg L⁻¹) to leucaena crude extract (370 mg eq BSA L⁻¹) and Fe₃O₄ (50 mg L⁻¹) (b)

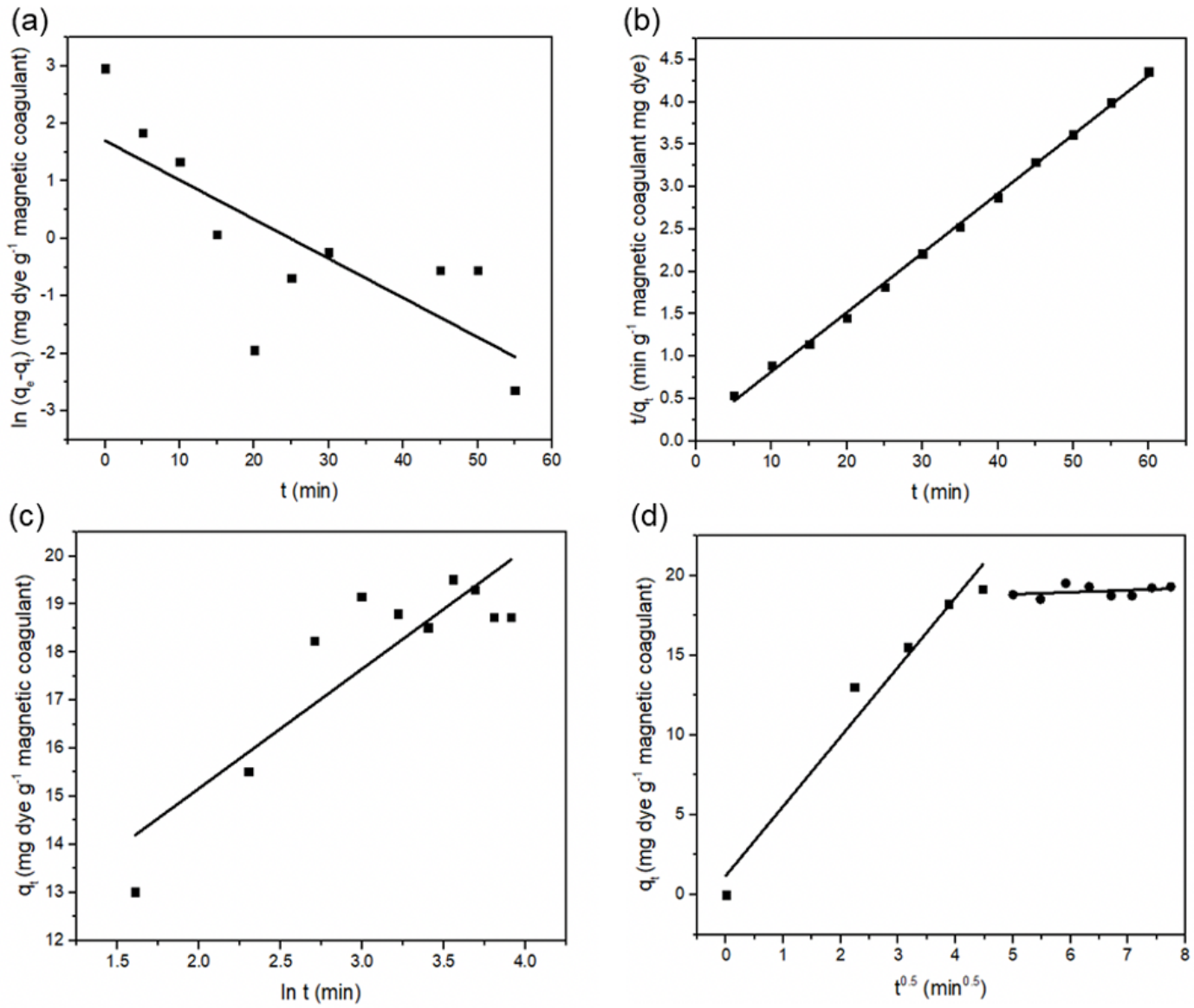


Figure 6

Plots of pseudo 1st order (a), pseudo 2nd order (b), Elovich (c), and inter-particle diffusion (d) kinetic model (pH 3, magnetic coagulant dosage 420 mg L⁻¹)

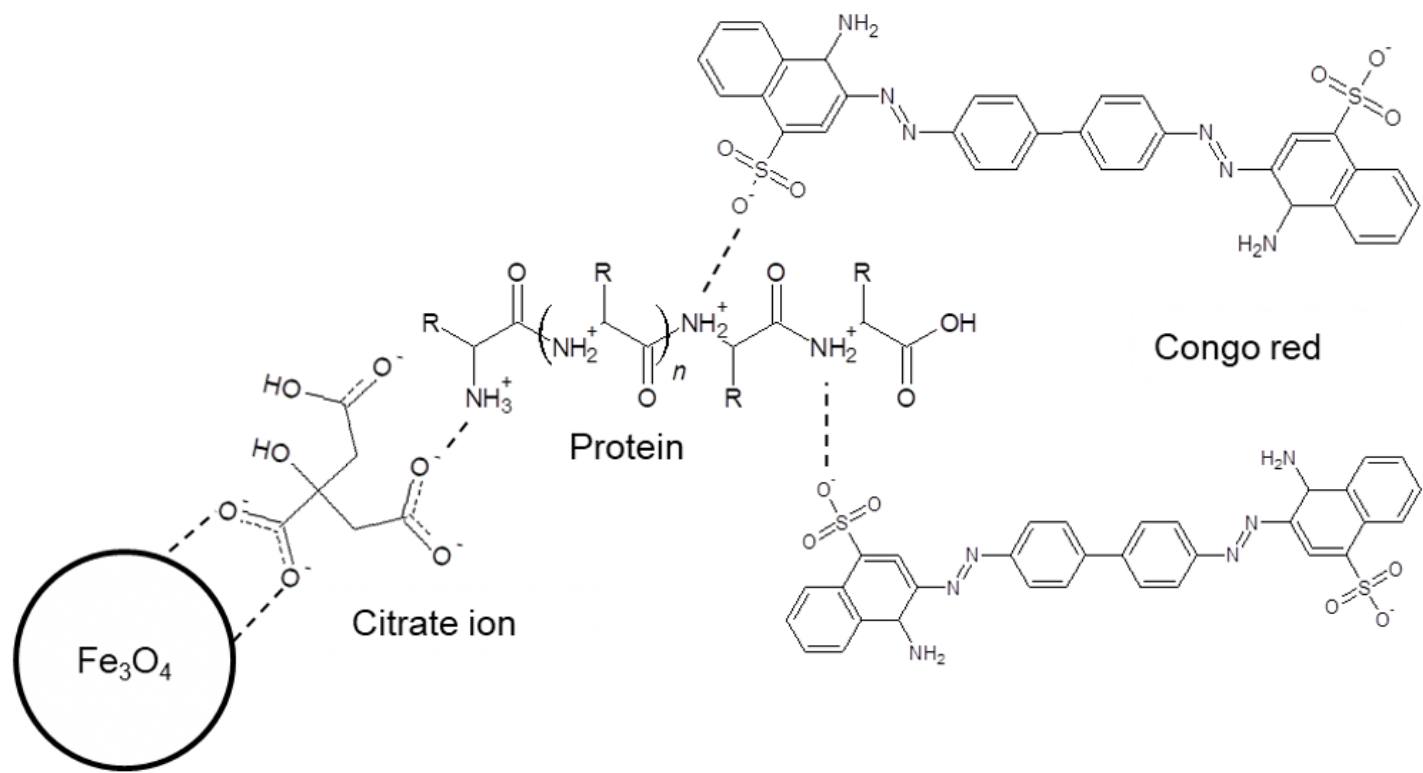


Figure 7

Illustration of Fe_3O_4 -CA and protein interaction and charge neutralization coagulation of Congo red